

Functional properties of a truncated recombinant GIRK5 potassium channel

Carolina Salvador ^a, Martin Martinez ^b, S. Ivonne Mora ^a, Waskar Egido ^a, Jose M. Farias ^b, Gerardo Gamba ^c, Laura I. Escobar ^{a,*}

^a Departamento de Fisiología, Facultad de Medicina, Universidad Nacional Autónoma de México, AP 70-250, México, D.F., Mexico

^b Departamento de Fisiología, Instituto Nacional de Cardiología Ignacio Chávez, México, D.F., Mexico

^c Unidad de Fisiología Molecular, Instituto de Ciencias Médicas y Nutrición Salvador Zubirán and Instituto de Investigaciones Biomédicas, Universidad Nacional Autónoma de México, AP 70-250, México, D.F., Mexico

Received 27 October 2000; received in revised form 8 March 2001; accepted 8 March 2001

Abstract

Xenopus laevis oocytes codify a G-protein-activated inward rectifier potassium channel (GIRK5 or Kir3.5). Coinjection of other GIRKs, the muscarinic m₂ receptor, or G $\beta\gamma$ protein cRNAs is required to observe functional GIRKx-GIRK5 heteromultimers in oocytes. Studies with GIRK2 isoforms have shown that the size of the amino or carboxyl terminus plays a crucial role on giving functional K⁺ channels. In this work we studied the properties of a GIRK5 with 25 amino acids deleted toward its amino-terminal domain. Injection of GIRK5-Δ25 cRNA alone displayed large basal and transient inward rectifying currents in oocytes. The instantaneous currents reached a stationary level after a long duration voltage pulse (10 s). For this relaxation, fast (τ_1) and slow (τ_2) time constants were estimated at different voltages. Recovery from inactivation followed a monoexponential function ($\tau = 0.95 \pm 0.07$ s). By contrast with other inward rectifier channels, blockade of GIRK5-Δ25 by extracellular Ba²⁺ was voltage-independent ($K_d = 102 \pm 2$ μ M), suggesting the presence of a Ba²⁺ site at the external channel vestibule. To confirm this hypothesis, the Ba²⁺ sensitivity of two charged mutants GIRK5-Δ25(N129E) and GIRK5-Δ25(K157E) at each of the external loops was determined. GIRK5-Δ25(N129E) and GIRK5-Δ25(K157E) showed a 100-fold and 2-fold higher affinity to Ba²⁺, respectively, supporting the existence of this Ba²⁺ binding site. © 2001 Published by Elsevier Science B.V.

Keywords: Inward rectifying potassium channel; Barium; G-protein activated channel; *Xenopus* oocyte

1. Introduction

The G-protein-activated inwardly rectifying K⁺ channels (GIRK or Kir3 subfamily) are critical mediators of cell excitability and effectors of many G-protein-coupled receptors [1]. For example, acetyl-

choline binds to cardiac muscarinic receptors (m₂) and then activates I_{KACH}, slowing heart rate. This atrial channel exists as a heteromultimer composed of two GIRK1 and two GIRK4 subunits [2]. So far the GIRK conducting K⁺ channels have been observed as an aggregation of two different GIRK subunits. GIRK2 and GIRK3 are found in the brain where they possibly form heteromeric channels with GIRK1. Coexpression of GIRK1 and GIRK2 produces functional channels in *Xenopus* oocytes like the

* Corresponding author. Fax: +52-5-623-2241;
E-mail: laurae@servidor.unam.mx

native G-protein-coupled inward rectifiers found in brain [3]. In contrast, some GIRK2 isoforms and GIRK4 alone also form functional G $\beta\gamma$ -gated homomultimers in various heterologous expression systems [2–5]. The mutants GIRK1(F137S) and GIRK4(S143T) form homomeric functional channels with activity comparable to the wild-type heteromeric G-protein-gated channels [6].

Alternative splicing at the 3'-end of the open reading frame of GIRK3.2 cRNA generates the four isoforms GIRK3.2a, GIRK3.2b, GIRK3.2c and GIRK3.2d [7–9]. GIRK3.2d is 18 amino acids shorter at the N-terminal end than of Kir3.2c and can form functional channels. In contrast, Kir3.2c can only form functional GIRK channels with GIRK-3.2a or GIRK3.1 [9]. It has been stated that both the N- and C-terminal ends of Kir3.2 isoforms play complex roles in the regulation of channel activity in GIRK channels composed of homomeric assemblies of GIRK3.2 isoforms [9].

The GIRK5 (Kir3.5) has been cloned from *Xenopus laevis* oocytes, the most widely used expression system [10]. Oocytes overexpressing GIRK5 in the absence of GIRK1 show very small Ach-stimulated currents [10]. The GIRK5 gene has three in-frame ATGs which could give rise to three GIRK5 proteins with different N-terminal sizes [10]. Whether all or some of these GIRK5 isoforms are synthesized in vivo is still an open question.

A small endogenous inward rectifying K $^{+}$ current (Xir) can be recorded in some *Xenopus* oocytes [11,12]. Therefore, we suspected that Xir could comprise an assembly of GIRK5 isoforms. To establish the functionality of likely GIRK5 isoforms derived from oocytes, we isolated by RT-PCR a GIRK5 homologue that was 25 amino acids shorter at its N-terminal end (GIRK5-Δ25). Oocytes injected with cRNA for GIRK5-Δ25 expressed large basal currents in the absence of coexpressed muscarinic receptor (i.e. m2) or G-protein subunits.

GIRK5-Δ25 channels displayed an instantaneous component with a prolonged inactivation profile (10 s) at high K $^{+}$ without Na $^{+}$. GIRK5-Δ25 channels were also blocked by extracellular Ba $^{2+}$ in a voltage-independent manner. In order to study the GIRK5-Δ25 Ba $^{2+}$ binding site, we focused on the possible electrostatic interaction between Ba $^{2+}$ and two amino acid residues at the external loops of GIRK5-Δ25.

Therefore, we mutated to the negatively charged residue glutamate (E) the amino acids N129 and K157. We obtained a decrease by two orders of magnitude in the K_d for Ba $^{2+}$ block with the GIRK5-Δ25(N129E) mutant. By contrast, GIRK5-Δ25(K157E) had only a slight change in its K_d . These results suggest that the amino acid residue position in the vestibule of a Kir channel is crucial in the electrostatic interaction with Ba $^{2+}$.

Preliminary results of this study were presented in abstract format [12].

2. Materials and methods

2.1. Molecular biology

Total RNA was obtained from 0.8 g of defolliculated *Xenopus* oocytes following the cesium chloride method [13]. RT-PCR experiments were performed to synthesize cDNA from 5 μ g total RNA (M-MLV reverse transcriptase, Gibco). Two primers were designed based on the amino acid sequence homology with GIRK4 and the GIRK5 clone previously isolated from *X. laevis* oocytes [10]. The nucleotide sequences for these primers (Gibco) were: 5'-CAT CGT CGA CAT GGC AAG GGA TTT AAG GGT CTC TAT G-3' (sense) and 5'-GAA ATG TAT CAA TGT TTT TCT GCA GTC AGT CTG GCT GTG-3' (antisense). A 1214 bp fragment was amplified by PCR either with the *Taq* polymerase (Gibco) or the High Expand enzyme (Boehringer Mannheim). The same result was obtained with the RNA from other frogs ($n=3$). The fragment was purified from an agarose gel (1%) by the Gene Clean method and subcloned in the pRSSP6013A3-UWE vector, pBF. DH5 α cells were transformed. The full GIRK5 codifying region was amplified by PCR with the primers 5'-AAA GGT CGA CAT GAT TCC TGA AAG AAT GGC-3' (sense) and 5'-AGA GAC CAA AAA GAG ACG ATC GTC GCC TGT ATC AAA G-3' (antisense). The fragment (300 bp) and the PBF-GIRK5-Δ25 construct were incubated with *Sa*I and *Xho*I. Ligation was performed with T4 DNA Ligase (Gibco). Purified DNAs (Maxi-prep, Qiagen) were sequenced automatically (AB1 Prism 310, Perkin Elmer) and manually (thermo-sequenase, Amersham Life Science).

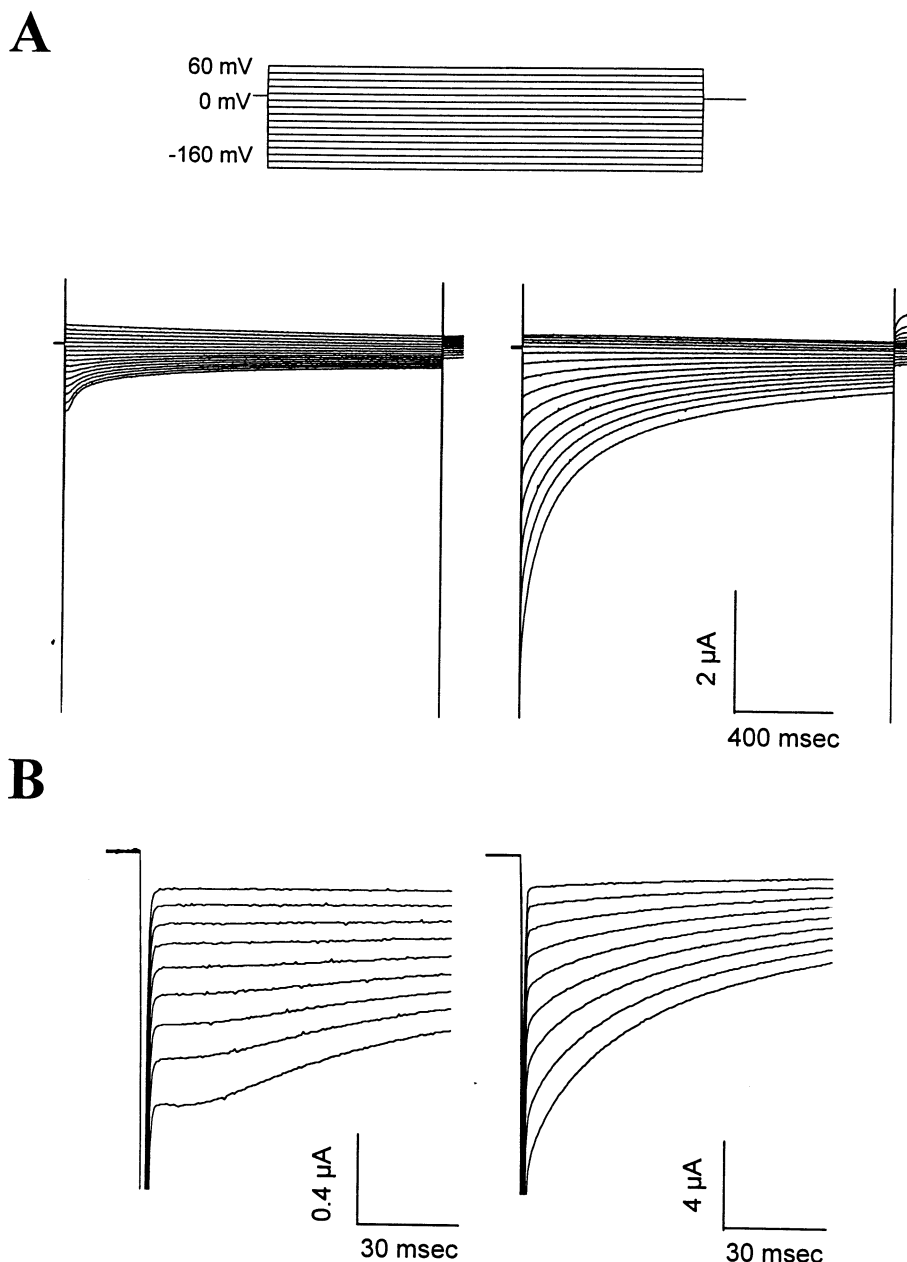


Fig. 1. (A) Current traces were recorded in high K^+ (118 mM) solutions for injected *Xenopus* oocytes with GIRK5 (left) and GIRK5- Δ 25 cRNAs (right). Voltage pulses from -160 to 60 mV were applied during 1500 ms with increments of 15 mV. The pulse protocol is shown at the top of the figure. The HP was set at 0 mV to inactivate most of the endogenous voltage-dependent ion channels. Traces are shown without subtracting linear components. (B) The above traces are shown with a different scale (vertical bar represents 0.4 and 4 μ A for GIRK5 and GIRK5- Δ 25 currents, respectively) during the first 100 ms. Inward currents were recorded from oocytes after 2 days of injection (10 ng of cRNA).

5–20 ng of GIRK5 wild-type and GIRK5- Δ 25 cRNA transcribed in vitro (RNA polymerase SP6, Gibco) were injected into oocytes for electrophysiological assays.

X. laevis females were purchased from Carolina Biological Supply Company, USA. Defolliculated oocytes were obtained according to [14].

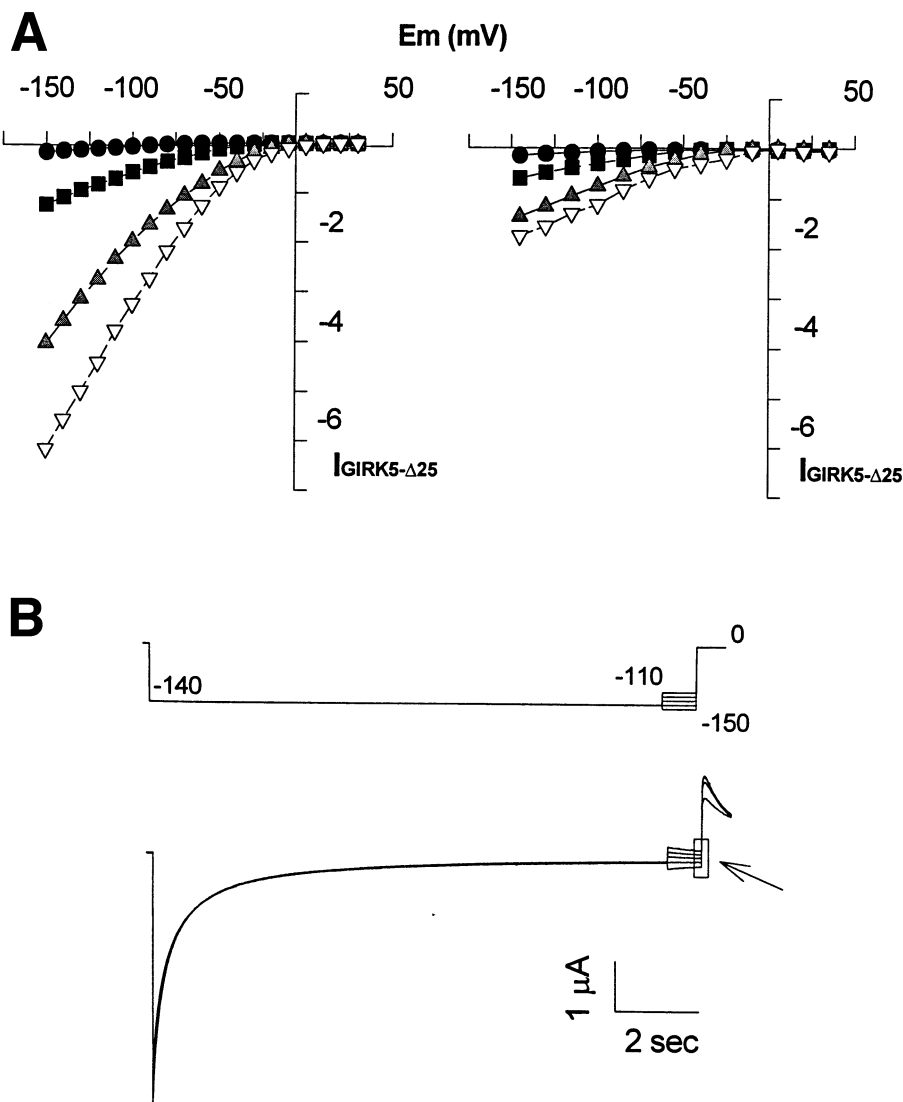


Fig. 2. I-V relationship of GIRQ5- Δ 25. (A) The current-voltage relationships are shown for the instantaneous current (left) and for the current at the end of the pulse (270 ms, right) at different external K^+ concentrations (118 (∇), 75 (\blacktriangle), 50 (\blacksquare) and 20 (\bullet) mM). The instantaneous component of the current was the value measured when the slope of capacitive current changed. This figure illustrates the substantial decay of GIRQ5- Δ 25 currents with time. Long pulses (>11 s), were required in order to reach the steady-state current level. (B) The protocol that was applied to subtract the leak current is shown at the top. The inward currents were measured with a long pulse (13 s) at -140 mV to inactivate completely the GIRQ5- Δ 25 channels. Then, several current traces were registered from -150 to -110 mV with 10 mV steps to develop only leak currents. The linear part of these traces allowed an estimate of the membrane resistance; the leak current was then subtracted off-line from the experimental data.

2.2. Electrophysiological assays

Recordings were made 1–3 days after cRNA injection, with a two-microelectrode voltage-clamp technique (Geneclamp 500, Axon Instruments). Borosilicate microelectrodes were filled with 3 M KCl and had resistances of 0.5–5 M Ω . Membrane potential and current signals were digitized at a rate of 10

kHz with a 12-bit AD/DA converter (TL-1 Labmaster, Axon Instruments) and filtered through a four-pole low-pass Bessel filter at a frequency of 2–5 kHz. Membrane potential and current signals were stored and analyzed off-line in a Pentium PC with pCLAMP v. 6.0, Microsoft Excel v. 2000 and Sigma-Plot, v. 2.0. Pooled data were expressed as mean \pm S.E. Unless otherwise indicated, current

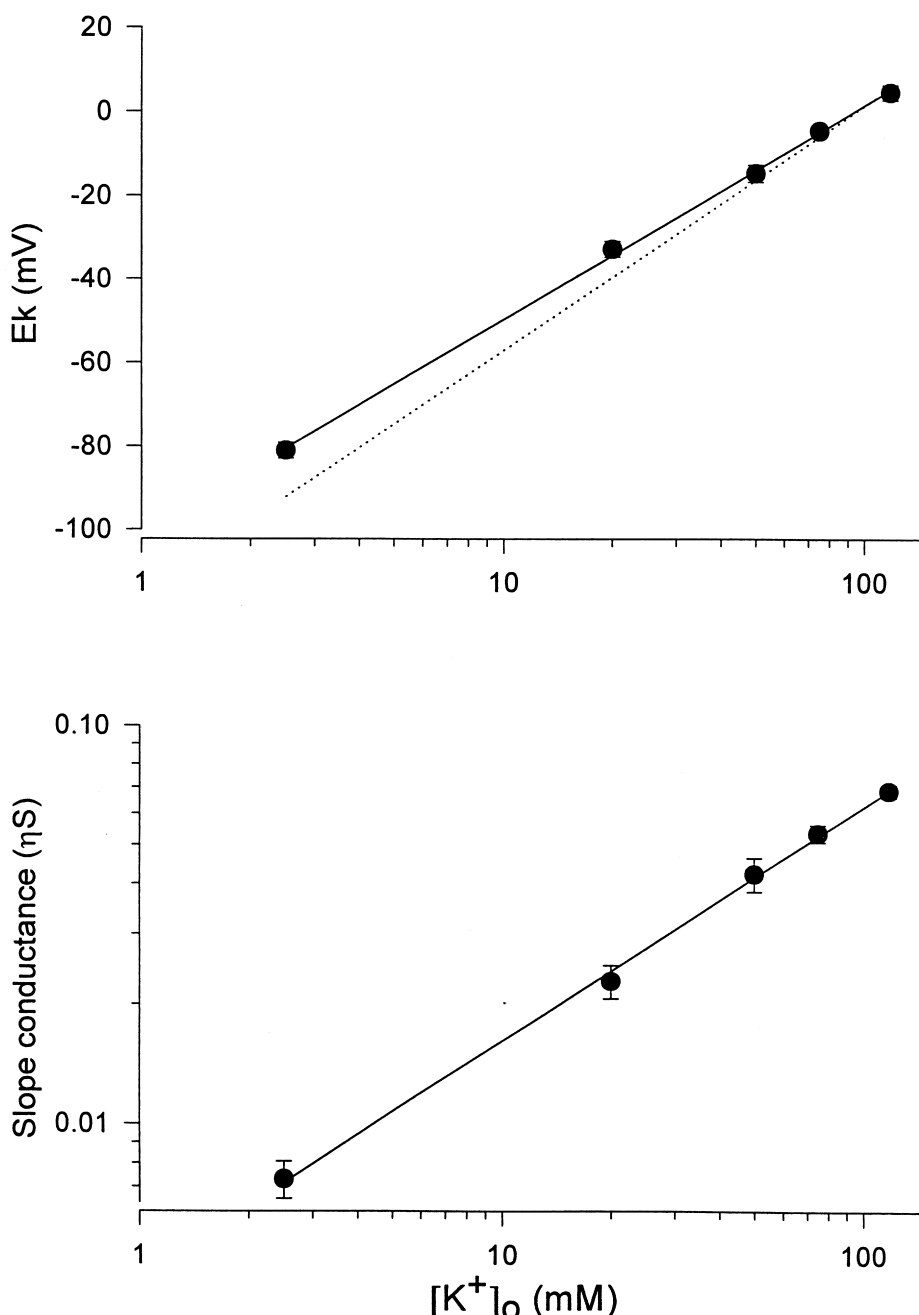


Fig. 3. Selectivity and permeation properties of GIRK5-Δ25. (Top) E_k as a function of $[K^+)_o$. Continuous line represents the linear regression fit to the experimental data; the fitted slope was 50.0 ± 2.9 mV. Dotted line indicates the Nernst equation prediction with a slope of 58 mV for a K^+ selective electrode. (Bottom) The slope conductance as a function of $[K^+)_o$. The linear regression fit (continuous line) had a slope of 0.586.

traces are shown after subtraction of the linear components. The leak component was subtracted off-line with a protocol applied after a long pulse to obtain only leak current (Fig. 2A, see legend for details). All

experiments were carried out at room temperature (22–24°C). Oocytes were placed in a 1 ml chamber and perfused with solution. Electrode impalement and measurement of oocyte passive properties were

Table 1

Comparison of the time constants for the fast (τ_1) and the slow (τ_2) components of GIRQ5-Δ25 and mutants

E_m (mV)	GIRQ5-Δ25		GIRQ5-Δ25(N129E)		GIRQ5-Δ25(K157E)	
	τ_1 (ms)	τ_2 (ms)	τ_1 (ms)	τ_2 (ms)	τ_1 (ms)	τ_2 (ms)
-160	55.07 ± 0.36	465.91 ± 19.6	50.06 ± 1.15	554.20 ± 12.2	59.90 ± 1.23	486.52 ± 17.6
-145	60.04 ± 0.76	476.04 ± 16.9	70.88 ± 0.23	543.48 ± 17.4	64.46 ± 2.23	476.91 ± 21.6
-130	69.33 ± 0.84	502.54 ± 21.1	78.44 ± 0.45	518.35 ± 23.4	72.95 ± 2.34	516.06 ± 19.2
-115	74.31 ± 1.49	509.19 ± 33.6	77.71 ± 1.12	484.46 ± 39.9	78.68 ± 5.76	535.95 ± 53.6
-100	82.40 ± 3.45	529.58 ± 39.8	95.67 ± 7.56	443.14 ± 82.7	92.11 ± 6.22	552.02 ± 62.5

The relaxation was measured in 118 mM [K⁺]_o ($n=3$; mean ± S.E.).

performed in normal Ringer solution (mM): NaCl 117, KCl 2.5, CaCl₂ 1.8, HEPES 5, pH 7.4. For selectivity experiments, Na⁺ was replaced with variable K⁺ concentrations (2.5, 20, 50, 75, and 118 mM). Functional expression of GIRQ5 and GIRQ5-Δ25 was studied in high K⁺ (118 mM).

3. Results

3.1. Isolation of GIRQ5-Δ25 from *X. laevis* oocytes

Since the GIRQ5 gene had been already cloned [10], the easiest step to obtain a truncated variant was by RT-PCR. To overcome the intrinsic problems of this technique, we worked with three independent total RNA samples derived from different frogs. In our study primers were designed to amplify the coding sequence from the third start codon of the GIRQ5 cDNA previously reported [10]. We obtained the GIRQ5 cDNA and GIRQ5 with 25 amino acids deleted at the N-terminal domain, GIRQ5-Δ25. We sequenced the three clones isolated from different frogs. Based on the same oligonucleotide sequence of these samples, using either the *Taq* polymerase or the more reliable High Expand enzyme, we concluded that no artifactual variants were amplified with this procedure.

In comparison with the GIRQ5 channel previously cloned [10], the GIRQ5-Δ25 isolated in this work showed an arginine at position 429 instead of a leucine and a lack of a glycine at position 430 at the end of the intracellular carboxyl domain. One clone out of three had a threonine at position 190 instead of an isoleucine in the M2 domain. These results suggest that the GIRQ5 gene displays polymorphism.

3.2. Functional expression in oocytes

Variable amounts of GIRQ5-Δ25 cRNA (5–20 ng) were injected into oocytes, yielding an approximately linear relationship between the amount of cRNA injected and the current observed (not shown). Inward inactivating currents were recorded in high K⁺ (118 mM; Fig. 1) at the second day with an injection of 10 ng of GIRQ5-Δ25 cRNA. Oocytes expressing inward potassium currents higher than 5 μA were used for recording. GIRQ5-Δ25 homomultimers showed an instantaneous current that decayed slowly to a steady state and increased in amplitude with the hyperpolarizing pulse.

If the GIRQ5-Δ25 activity were caused by its association with the endogenous oocyte GIRQ5 subunit and if subunits associated more or less randomly in all possible combinations, one would expect less current with higher amounts of GIRQ5-Δ25 cRNA or during longer times of channel expression over a relatively constant background of endogenous GIRQ5. As shown in Fig. 1B, this is not the case. As more GIRQ5-Δ25 cRNA was injected more current was measured. This also happened with the recording time (3–4 days after injection). We have also injected the GIRQ5 wild-type cRNA (i.e. the full gene) into the oocytes, and inward currents were not observed under the same conditions (not shown).

3.3. K⁺-dependent activation and permeation properties of GIRQ5-Δ25 homomultimers

I-V relationships for the instantaneous currents and for the currents at the end of the 10 s pulse were estimated for GIRQ5-Δ25 channels in variable [K⁺]_o (Fig. 2). Whole-cell currents were recorded in 2.5, 20, 75 and 118 mM [K⁺]_o. Currents were elicited

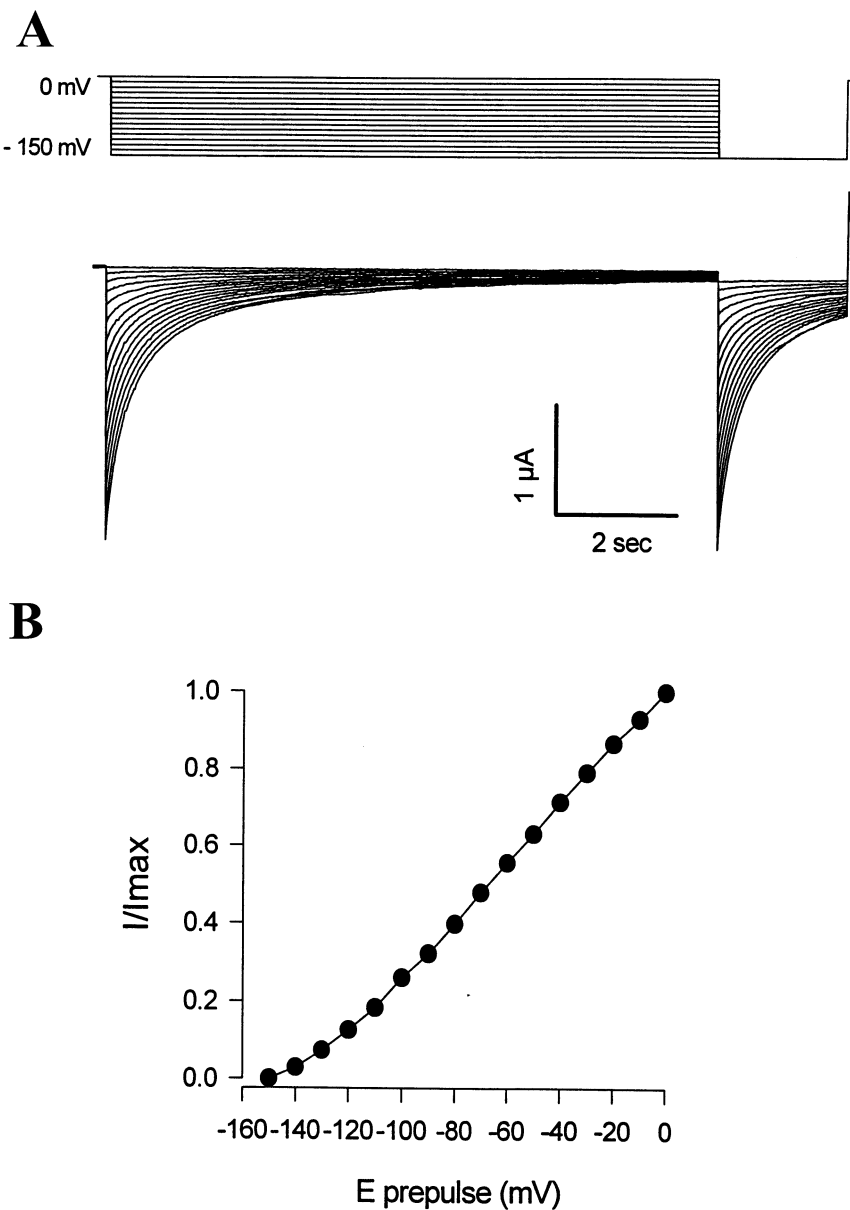


Fig. 4. Steady-state inactivation of the inward rectifying K^+ current. (A) Traces show unsubtracted membrane currents elicited with the pulse protocol shown at the top, in 118 mM $[K^+]_o$. (B) The steady-state inactivation induced by a 10 s prepulse was evaluated measuring the instantaneous current at the test pulse (-150 mV) and plotted as a function of the prepulse potential (see text for more details).

from a holding potential (HP) of 0 mV, with the pulse protocol shown at the top of Fig. 1. Off-line subtraction of leak currents was performed with the protocol shown in Fig. 2B (for details see figure legend). Like other inward rectifier potassium channels, the current amplitude of GIRK5-Δ25 channels was dependent on the $[K^+]_o$ at all voltages and the I-V curves were shifted with respect to $[K^+]_o$.

The zero current potential was calculated for each I-V curve at all $[K^+]_o$ ($n=3$) and it was compared with the value predicted by the Nernst equation (Fig. 3, top). The experimental points were very close to the ones estimated except for concentrations lower than 20 mM. Endogenous Na^+ and Cl^- currents may become apparent in the oocytes at low $[K^+]_o$. The linear regression fit of the data in a semilog-

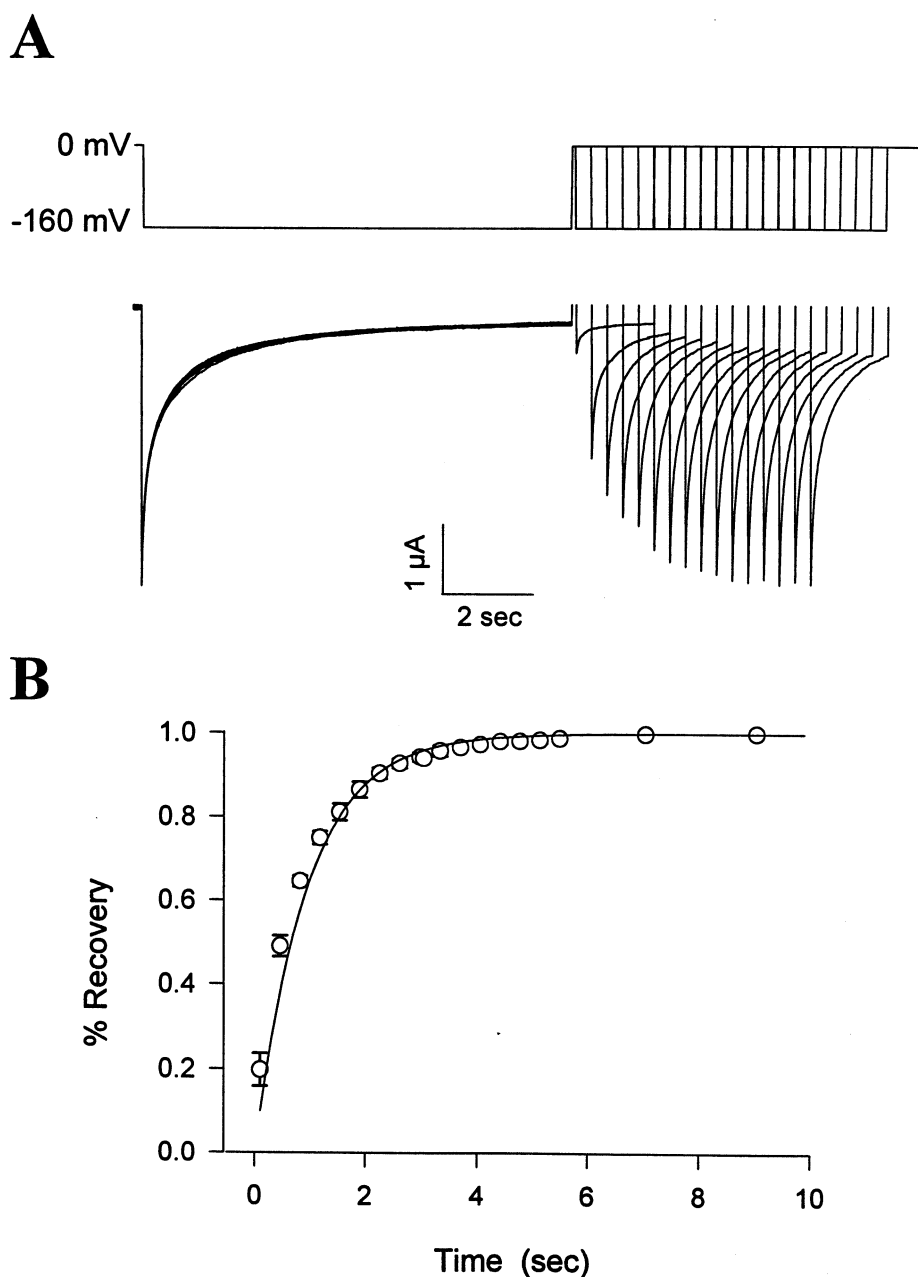


Fig. 5. Recovery from the voltage-dependent inactivation. (A) Time course of the recovery at 0 mV from the steady-state inactivation after a prepulse (9 s) to -160 mV. The recovery was evaluated from the instantaneous current elicited by a test pulse to -160 mV applied at progressive periods (between 10 and 10 000 ms) after the conditioning prepulse. (B) Instantaneous current recovery as a function of the interval duration. Data were fitted to a monoexponential function with $\tau_i = 0.95$ ms.

rithmic scale had a slope value of 50.0 ± 2.9 mV, close to the 58 mV/decade change in $[K^+]_o$ for a K^+ selective electrode (dotted line), indicating that GIRQ5-Δ25 channels were mainly selective for potassium ions.

Fig. 3 (bottom) shows the conductance depen-

dence of GIRQ5-Δ25 channels on $[K^+]_o$. The slope conductance was determined by fitting the linear part (between -150 and -70 mV) of the instantaneous I-V curve at the different $[K^+]_o$ and plotted in a double logarithmic scale. This relationship was well described by the power function $g_{slope} = A ([K^+]_o)^{0.586}$, where

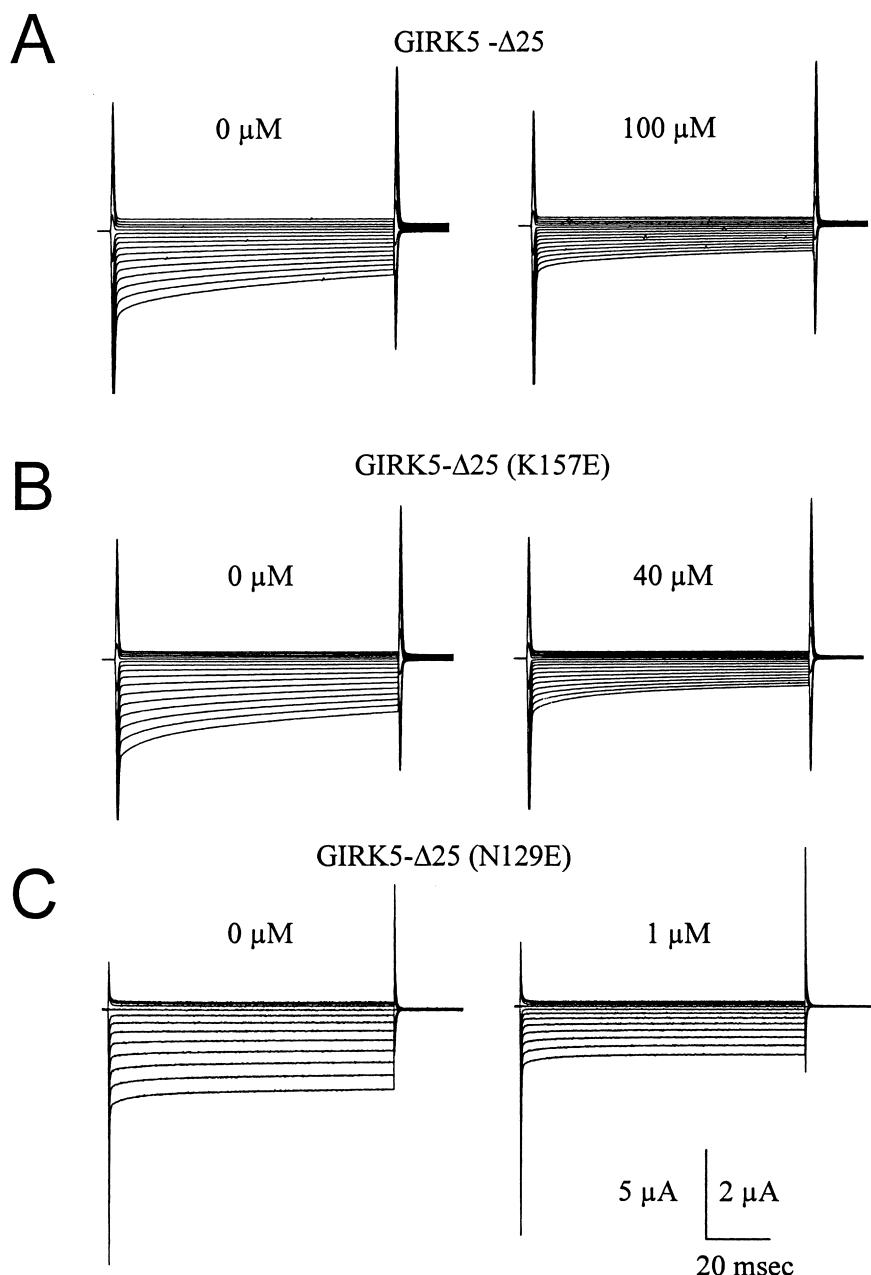


Fig. 6. Effect of charge in the sensitivity of GIRK5-Δ25 to Ba^{2+} block. (A,B,C) Whole oocyte GIRK5-Δ25, GIRK5(K157E) and GIRK5-Δ25(N129E) currents in the absence and presence of 100, 40 and 1 μM BaCl_2 . Currents were recorded and analyzed as indicated in Fig. 1.

$A = 0.36 \pm 0.13 \text{ nS}$, $[\text{K}^+]_o$ is in mM and 0.586 is the slope of the linear regression line. This value was close to 0.5, indicating that the conductance was approximately proportional to the square root of $[\text{K}^+]_o$, which is typical of an inward rectifier potassium channel [15].

3.4. Voltage-dependent inactivation

In general, the small decay of Kir currents before they reach the steady state has been attributed to a combination of extracellular K^+ depletion, external Na^+ blockade, and a voltage-dependent inactivation [15–17].

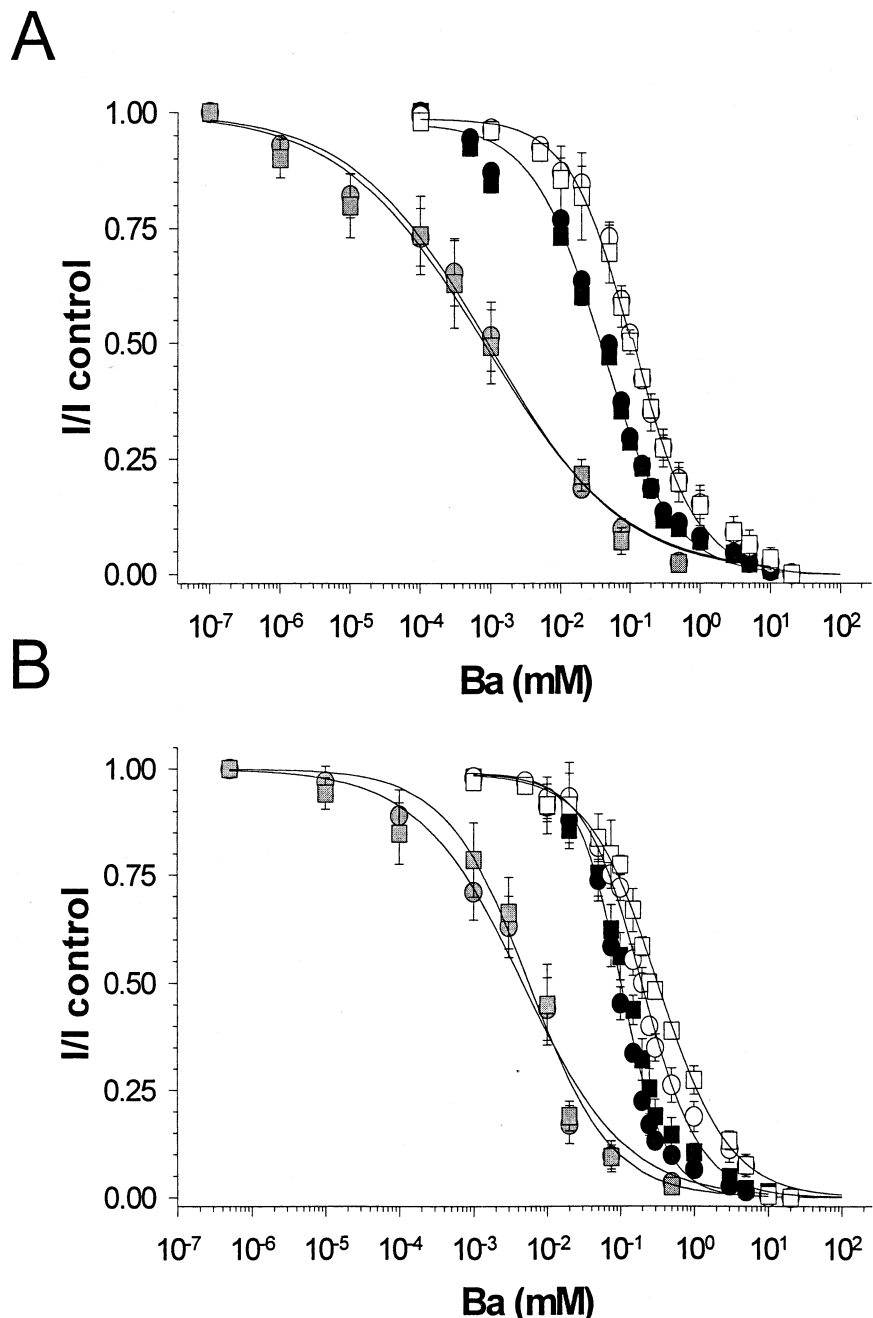


Fig. 7. Sensitivity and voltage independence of GIRQ5-Δ25 and the charge mutants GIRQ5-Δ25(K157E) and GIRQ5-Δ25(N129E) to Ba²⁺ block. Effect of Ba²⁺ on the instantaneous (A) and the late current at 750 ms (B) of GIRQ5-Δ25, GIRQ5-Δ25(N129E) and GIRQ5-Δ25(K157E) (empty, gray and filled symbols, respectively) at two voltages, -160 mV (squares) and -80 mV (circles). Recordings were performed in 118 mM of [K⁺]_o at several Ba²⁺ concentrations. The pulse protocol was the same as in Fig. 1. Mean \pm S.E. values of unblocked current fraction (I/I_{control}) were plotted at -160 and -80 mV ($n=5$) as a function of Ba²⁺ concentration.

GIRQ5-Δ25, GIRQ5-Δ25(K157E) and GIRQ5-Δ25(N129E) currents showed a prominent decay at test potentials negative to -50 mV even at high [K⁺]_o with nominally zero [Na⁺]_o (Table 1). We

studied this process with a standard inactivation protocol of two pulses shown in Fig. 4A. Prepulses to selected membrane potentials between -150 and 0 mV from a HP of 0 mV were applied during 10 s

Table 2

Voltage dependence of GIRK5-Δ25, GIRK5-Δ25(K157E) and GIRK5-Δ25(N129E) to Ba²⁺ blockade

	−160 mV (μM)	−80 mV (μM)
<i>I inst</i>		
GIRK5-Δ25	111.35 ± 7.13	107.62 ± 6.16
GIRK5-Δ25(K175E)	43.83 ± 3.74	39.52 ± 4.0
GIRK5-Δ25(N129E)	1.74 ± 0.77	2.01 ± 1.36
<i>I late</i>		
GIRK5-Δ25	188.45 ± 12.78	330.23 ± 26.45
GIRK5-Δ25(K157E)	95.75 ± 3.40	119.06 ± 6.01
GIRK5-Δ25(N129E)	5.65 ± 1.95	7.20 ± 1.92

K_d values (μM) were estimated at −160 and −80 mV for the instantaneous (*I inst*) and late currents (750 ms) from Fig. 7 (mean ± S.E.).

to allow the current to reach the steady state (I_{ss}). The peak current elicited at the test pulse of −150 mV and after subtracting I_{ss} was normalized to the maximal current observed without prepulse (I/I_{max}), to determine the steady-state inactivation. A sigmoidal relationship was observed, revealing the fraction of channels that was not inactivated at the different prepulse potentials (Fig. 4B). Complete inactivation was observed when prepulses were more negative than −150 mV during 10 s test pulses. These recordings were performed at high [K⁺]_o without Na⁺.

The recovery time course at 0 mV from the inactivation of GIRK5-Δ25 at −160 mV (Fig. 5A) was determined using a standard two-pulse protocol (upper part). The inactivating prepulse to −160 mV was followed by increasing recovery periods at 0 mV preceding the −160 mV test pulse. The instantaneous current at the onset of the test pulse was compared and normalized with the current obtained at the prepulse. These data were plotted as a function of time (Fig. 5B). The time course of the recovery at 0 mV could be fitted by a monoexponential function with a time constant of 0.95 ± 0.07 s ($n = 4$). In other Kir channels this recovery also follows a monoexponential time course [18].

3.5. Sensitivity to Ba²⁺ blockade

The high sensitivity to barium blockade is one pharmacological property of Kir channels and K_d values between 10 and 500 μM have been reported [14,19,24]. Families of GIRQ5-Δ25, GIRQ5-Δ25(N129E) and GIRQ5-Δ25(K157E) current traces

were recorded in 118 mM of [K⁺]_o at variable concentrations of external Ba²⁺ (Fig. 6). The current amplitude at the onset and at the end of the pulse became smaller with increasing [Ba²⁺]_o (Fig. 6). This blockade could be readily reversed by removal of Ba²⁺ from the external solution (not shown).

In several Kir channels, Ba²⁺ blocks the steady-state current rather than the peak current, and this blockade is a voltage-dependent process [15,20,25]. In GIRQ5-Δ25 and GIRQ5 mutants, Ba²⁺ affected more importantly the instantaneous current amplitude rather than the current at the end of the pulse ('late current') (Figs. 6 and 7, Table 2).

Usually extracellular Ba²⁺ preferentially affects Kir channels at more negative potentials. For example, the Kir2.1 potassium channel has a high Ba²⁺ sensitivity: $E_m = -160$ mV, $K_d = 0.2$ μM; $E_m = -80$ mV, $K_d = 2.2$ μM [25]. By contrast, GIRQ5-Δ25 displayed a voltage-independent Ba²⁺ blockade: K_d values of 111.4 ± 7.1 and 107.6 ± 6.2 μM at −160 and −80 mV were determined, respectively. In order to explain the difference in Ba²⁺ sensitivity between these Kir subfamilies, we focused on the electrostatic interaction between Ba²⁺ and two amino acid residues at the external loops of GIRQ5-Δ25. Therefore, we mutated to the negatively charged residue glutamate (E) the amino acids N129 and K157 for the following reasons: the negative glutamate residue (E117) in Kir2.1, present in its first loop, has a crucial role in single channel conductance and Ba²⁺ affinity [26]. The corresponding amino acid residue in GIRQ5-Δ25 is the neutral amino acid residue asparagine (N129). To study the impact of changing only the charge at the GIRQ5 vestibule, we mutated the

positive amino acid residue lysine K157 in the second external loop of GIRQ5-Δ25 to glutamate (E).

Current-voltage relationships were determined in 118 mM K⁺ containing Ba²⁺ from 0.001 to 20 mM ($n=5$; Fig. 7). The blocked fractions (I/I_{max}) for the instantaneous and late currents were measured at all voltages. GIRQ5-Δ25 showed a $K_d = 102 \pm 2 \mu\text{M}$ and a $K_d = 227 \pm 9 \mu\text{M}$ for Ba²⁺ blockade at the instantaneous and late current, respectively.

We obtained a change of about two orders of magnitude in the K_d for Ba²⁺ with the GIRQ5-Δ25(N129E) mutant ($K_d = 1.8 \pm 0.5 \mu\text{M}$). By contrast, the GIRQ5-Δ25(K157E) mutant was only 2-fold more sensitive to Ba²⁺ blockade ($K_d = 41.7 \pm 3.5$; Fig. 7, Table 2). Therefore, the amino acid residue position in the vestibule of a Kir channel is crucial in a possible electrostatic interaction with Ba²⁺.

Table 2 shows the K_d values for instantaneous and steady-state (late) currents, confirming the voltage independence of Ba²⁺ blockade for GIRQ5-Δ25 and the charge mutant channels (Fig. 7).

4. Discussion

An outstanding result of this work is that the GIRQ5 gene with a shorter N-terminal end, the GIRQ5-Δ25, gives rise to functional channels, in contrast with the lack of functionality observed with the GIRQ5 cRNA injected alone or with m2 and Gβγ cRNAs in *X. laevis* oocytes [10]. This result is in accordance with the functionality also observed with the GIRQ3.2d with a shorter N-terminal end [9].

The high basal activity of GIRQ5-Δ25 channels in the oocytes is intriguing. GIRQ1/GIRQ4 heteromultimers and some GIRQ2 isoforms express significant basal K⁺ currents without receptor stimulation or G-protein activation [6,9,22]. This activity has been related to the direct action of intracellular sodium ions, requiring ATP hydrolysis. The ATP dependence of GIRQ channel activity is mediated via phosphoinositol diphosphates (PIP₂). The presence of PIP₂ is essential not only for the channel gating by sodium ions but also for efficient Gβγ signaling [21,22]. Since channels work efficiently even at high expression levels in the oocytes, the endogenous pool of any of these gating molecules does not appear to be a limit-

ing factor for GIRQ5-Δ25 functionality. We have also observed functional GIRQ5-Δ25 homomultimers in an insect line but GTP-γS is required to allow for channel activity (not shown).

Inward rectifier potassium channels display only a small inactivation [15]. The inactivation of GIRQ5-Δ25 currents had a slow time course. So far two inactivation mechanisms have been described for voltage-dependent potassium channels: a fast process referred as ‘the ball and chain’ (N-type [23]) and a slow decaying current event that strongly depends on the channel pore structure (C-type [24]). Further studies should be performed to investigate the GIRQ5-Δ25 inactivation.

Ba²⁺ blockade of the GIRQ5-Δ25 instantaneous and late currents was voltage-independent (Fig. 7, Table 2), implying the existence of an external binding site. In other Kir channels, extracellular Ba²⁺ enhances dramatically the rate of current decay by entering and blocking their pores [14,16,24]. The presence of a Ba²⁺ binding site located outside the pore of the GIRQ5-Δ25 channels was tentatively confirmed by the higher affinity determined for the two charge mutants: GIRQ5-Δ25(N129E) and GIRQ5-Δ25(K157E). Furthermore, the 100-fold higher sensitivity of mutant GIRQ5-Δ25(N129E) for Ba²⁺ suggests that the first channel external loop contributes to the binding site for this blocker.

Important conclusions are derived from this work. First, GIRQ5 channels lacking the first 25 amino acids at the N-terminal end produce functional homomultimers with an appreciable basal activity suggesting a high sensitivity of this truncated channel to the endogenous activators (i.e. Gβγ proteins, Na⁺, Mg-ATP and PIP₂). Second, in contrast to other potassium channels, GIRQ5-Δ25 homomultimers present a prolonged inactivation and a voltage-independent Ba²⁺ blockade. The higher Ba²⁺ affinity of the mutant charge GIRQ5-Δ25(N129E) at the first loop of the channel vestibule supports the presence of an external Ba²⁺ site in GIRQ5 channels.

Acknowledgements

We thank Dr. Peter Ruppertsberg for the PBF vector; Dr. Ana Correa and Dr. Dick Horn for their careful reading of the manuscript. We thank Monica

Salas Garcia for technical assistance. This work was supported by DGAPA IN220199 and CONACYT 30570-M grants to LE, CONACYT 30882-M and CONACYT 27692m grants to MM and GG, respectively. GG is an International Research Scholar from the Howard Hughes Medical Institute.

References

- [1] N. Dascal, Signalling via the G protein-activated K⁺ channels, *Cell. Signal.* 9 (1997) 551–573.
- [2] G. Krapivinsky, E.A. Gordon, K. Wickman, B. Velimirovic, L. Krapivinsky, D.E. Clapham, The G-protein-gated atrial K⁺ channel I_{KACH} is a heteromultimer of two inwardly rectifying K⁺ proteins, *Nature* 374 (1995) 135–141.
- [3] B.M. Velimirovic, E.A. Gordon, N.F. Lim, B. Navarro, D.E. Clapham, The K⁺ channel inward rectifier subunits form a channel similar to neuronal G protein-gated K⁺ channel, *FEBS Lett.* 379 (1996) 31–37.
- [4] K.W. Chan, M.N. Langan, J.L. Sui, J.A. Kozak, A. Pabon, J.A. Ladis, D.E. Logothetis, A recombinant inwardly rectifying potassium channel coupled to GTP-binding proteins, *J. Gen. Physiol.* 107 (1996) 381–397.
- [5] P. Kofuji, N. Davidson, H.A. Lester, Evidence that neuronal G-protein-gated inwardly rectifying K⁺ are activated by G $\beta\gamma$ subunits and function as heteromultimers, *Proc. Natl. Acad. Sci. USA* 92 (1995) 6542–6546.
- [6] M. Vivaudou, K.W. Chan, J.L. Sui, L.Y. Jan, E. Reuveny, D.E. Logothetis, Probing the G-protein regulation of GIRK1 and GIRK4, the two subunits of the KACH channel. Using functional homomeric mutants, *J. Biol. Chem.* 272 (1997) 31553–31560.
- [7] F. Lesage, F. Duprat, M. Fink, E. Guillemin, T. Coppola, M. Lazdunski, J.P. Hugnot, Cloning provides evidence for a family of inward rectifier and G-protein coupled K⁺ channels in the brain, *FEBS Lett.* 353 (1994) 37–42.
- [8] S. Isomoto, C. Kondo, N. Takahashi, S. Matsumoto, M. Yamada, T. Takumi, Y. Horio, Y. Kurachi, A novel ubiquitously distributed isoform of GIRK2 (GIRK2B) enhances GIRK1 expression of the G-protein-gated K⁺ current in *Xenopus* oocytes, *Biochem. Biophys. Res. Commun.* 218 (1996) 286–291.
- [9] A. Inanobe, Y. Horio, A. Fujita, M. Tanemoto, H. Hibino, K. Inageda, Y. Kurachi, Molecular cloning and characterization of a novel splicing variant of the Kir3.2 subunit predominantly expressed in mouse testis, *J. Physiol.* 521 (1999) 19–30.
- [10] K.E. Hedin, N.F. Lim, D.E. Clapham, Cloning of a *Xenopus laevis* inwardly rectifying K⁺ channel subunit that permits GIRK1 expression of I_{KACH} currents in oocytes, *Neuron* 16 (1996) 423–429.
- [11] C.K. Bauer, T. Falk, J.R. Schwarz, An endogenous inactivating inward-rectifying potassium current in oocytes of *Xenopus laevis*, *Pflug. Arch. Eur. J. Physiol.* 432 (1996) 812–820.
- [12] M. Martinez, C. Salvador, S.I. Mora, G. Gamba, L. Escobar, Cloning and functional characterization of a Kir3 channel from *Xenopus* oocytes, *Biophys. J.* 76 (1999) S-P241, A73.
- [13] J. Sambrook, E.F. Fritsch, T. Maniatis, *Molecular Cloning. A Laboratory Manual*, 2nd edn., Cold Spring Harbor Laboratory Press, San Diego, CA, 1989, pp. 7.19–7.22.
- [14] B. Rudy, L.E. Iverson, *Methods Enzymol.* 207 (1992) 266–279; 270–274.
- [15] S. Hagiwara, S. Miyasaki, P. Rothenthal, Potassium current and the effect of cesium on this current during anomalous rectification of the egg cell membrane of a starfish, *J. Gen. Physiol.* 67 (1976) 621–638.
- [16] B. Sakman, G. Trube, Voltage-dependent inactivation of inward-rectifying single-channel currents in the guinea-pig heart cell membrane, *J. Physiol.* 347 (1984) 641–657.
- [17] N.B. Standen, P.R. Stanfield, A potential and time-dependent blockade of inward rectification in frog skeletal muscle fibres by barium and strontium ions, *J. Physiol.* 280 (1978) 169–191.
- [18] R.D. Harvey, R.E. Ten Eick, Characterization of the inward-rectifying potassium current in cat ventricular myocytes, *J. Gen. Physiol.* 91 (1988) 593–615.
- [19] S. Hagiwara, S. Miyasaki, W. Moody, J. Patlak, Blocking effects of barium and hydrogen ions on the potassium current during anomalous rectification in the starfish egg, *J. Physiol.* 279 (1978) 167–185.
- [20] Y. Kubo, T.J. Baldwin, Y.N. Jan, L.Y. Jan, Primary structure and functional expression of a mouse inward rectifier potassium channel, *Nature* 362 (1993) 127–132.
- [21] C. Huang, S. Feng, D.W. Hilgemann, Direct activation of inward rectifier potassium channels by PIP2 and its stabilization by G $\beta\gamma$, *Nature* 391 (1998) 803–806.
- [22] J.L. Sui, K.W. Chan, D.E. Logothetis, Na⁺ Activation of the muscarinic K⁺ channel by a G-protein-independent mechanism, *J. Gen. Physiol.* 108 (1996) 381–391.
- [23] T. Hoshi, W.N. Zagotta, R.W. Aldrich, Two types of inactivation in Shaker K⁺ channels: effects of alterations in the carboxy-terminal region, *Neuron* 7 (1991) 547–556.
- [24] J. Lopez-Barneo, T. Hoshi, S.H. Heinemann, R.W. Aldrich, Effects of external cations and mutations in the pore region on C-type inactivation of Shaker potassium channels, *Recept. Channels* 1 (1993) 61–71.
- [25] R. Shieh, J. Chang, J. Arreola, Interaction of Ba²⁺ with the pores of the cloned inward rectifier K⁺ channels Kir2.1 expressed in *Xenopus* oocytes, *Biophys. J.* 75 (1998) 2313–2322.
- [26] D.S. Navaratnam, L. Escobar, M. Covarrubias, J.C. Oberholzer, Permeation properties and differential expression across the auditory receptor epithelium of an inward rectifier K⁺ channel cloned from the chick inner ear, *J. Biol. Chem.* 270 (1995) 19238–19245.